AIAA xxx
Voltage Requirements for Electrostatic Inflation of Gossamer Space Structures

Laura A. Stiles, Hanspeter Schaub, and Kurt K. Maute

University of Colorado, Boulder, CO 80309-0431

AIAA Gossamer Systems Forum
April 4–7, 2011 / Denver, CO

Voltage Requirements for Electrostatic Inflation of Gossamer Space Structures

Laura A. Stiles,* Hanspeter Schaub,† and Kurt K. Maute‡

University of Colorado, Boulder, CO 80309-0431

This paper explores the concept of using electrostatic forces for actuation of gossamer space structures. The Electrostatically Inflated Membrane Structure (EIMS) uses two conducting membranes that are interconnected through ribs. An absolute electrostatic charge is given to the structure through active charge emission, causing repulsion between layers of lightweight membrane and leading to additional stiffness in the system. Of the dominant orbital perturbations considered for EIMS, the differential solar radiation pressure is found to have larger impact then the differential gravity forces due to the small, centimeter-level separation distance between the membranes. The minimum potentials required to compensate for differential solar radiation pressure at geostationary altitudes are determined to be on the order of hundreds of volts. Also addressed are challenges of electrostatic inflation of membrane structures in an Earth orbit environment, and preliminary results of experiments illustrating inflation on simple prototype structures are presented.

I. Introduction

Lightweight gossamer spacecraft structures provide an interesting alternative to the traditional mechanical systems which are typically more massive and expensive to launch. Many different applications of gossamer space hardware have previously been explored, and a select few have been successfully employed in space. Examples of early work in inflatable structures include the development of the mylar ECHO balloons in 1958 at NASA. The ECHO I sphere, which was launched in 1960, successfully served as a communications reflector in space for several months.[1] L'Garde Inc. made many early contributions to the field of deployable technology, including the support for NASA to the launch an inflatable antenna from the Space Shuttle.[2] Examples of present day gossamer spacecraft research include solar sail technology,[3] inflatable solar arrays,[4] and space habitats.[5]

Common methods for actuation of gossamer structures include inflation via pressurized gas, sublimating chemicals, or evaporating liquids.[6] This paper further explores a novel method for inflation of membrane space structures, described in Reference 7, which uses electrostatic repulsion to create the needed inflation forces. With no outside force for inflating or tensioning a structure, there is no rigidity or stiffness for maintaining a nominal desired shape or configuration. Applying electric charge to a layered gossamer structure provides an inflation pressure due to repulsive electrostatic forces between the charged layers, per Coulomb's law. Elements of the structure can self-repel with this applied potential, thus inflating to a more stiff structure, much like inflation of an airbag with gas. However, in contrast to gas-inflated structures, the electrostatically inflated structure does not suffer from sensitivities to membrane punctures. In fact, the simple concepts considered in this paper are open ended membrane structures resembling more the ribbed open structure of a ram-air parachute than that of a fully enclosed balloon. The electrostatic inflation idea is illustrated in Figure 1.

The electrostatic inflation concept is particularly applicable to structures such as arrays, solar power reflectors, or drag augmentation devices for de-orbiting and space debris avoidance purposes. In applying electrostatics for inflation

*Graduate Research Assistant, Aerospace Engineering Sciences Department, University of Colorado, Boulder, CO. AIAA student member, AAS student member

†Associate Professor, H. Joseph Smead Fellow, Aerospace Engineering Sciences Department, University of Colorado, Boulder, CO. AIAA Associate Fellow, AAS member

‡Associate Professor, H. Joseph Smead Fellow, Aerospace Engineering Sciences Department, University of Colorado, Boulder, CO

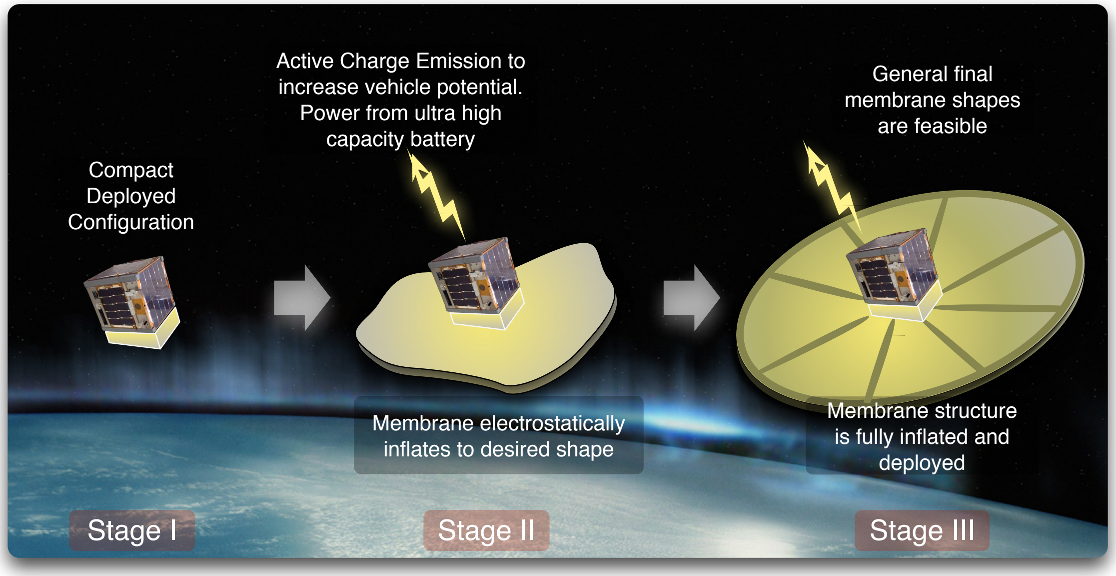

Figure 1: Electrostatic inflation concept

of these and other space apertures, there is the potential to significantly decrease mass, while reducing the associated deployment oriented power and packing volume for deployable structures. A large ratio of deployed volume to stowed volume is very advantageous, especially in highly volume-constrained spacecraft such as Nanosats or CubeSats. Many apertures have performance directly related to their deployed surface area while their design is limited by available pre-launch stowed volume.

The concept of electrostatics for control of space structures has been studied for many decades. The previous research has mainly focused on using electrostatics to precisely control the shape of membrane surfaces whose outer edges are held in place by a solid structure. A US patent by J.H. Cover filed in 1966 describes an invention for using electrostatics to control the surface of a reflector dish in space.[8] This patent also discusses how electrostatic forces can be created using active charge emission using only Watt levels of power at geosynchronous orbit altitudes. However, the electrostatics are only used to shape a single membrane. In contrast, the concept presented in this paper uses electrostatics to inflate a self-supporting layered membrane structure. Electrostatically controlling the surface of membrane mirrors in space has also been studied, an example of such is the work of Errico, et. al. in Reference 9. These designs significantly differ from the proposed membrane structure inflation as the mirror and reflector technology requires an external ring structure to support the surfaces. With inflation of the membrane structures, the gossamer structure is completely and compactly stowed until the charge level is increased to cause the entire structure to inflate.

Another field of related research is Coulomb control for proximity flying spacecraft. This application aims to raise the absolute potential of the spacecraft to control the electrostatic interactions with surrounding craft. Actively charging a craft to a few kilovolts causes electrostatic forces between the craft of micro- to milli-Newton levels with millisecond charging time.[10,11] In References 12 and 13 the Coulomb force is explored to develop static virtual structures subject to both to the gravitational and electrostatic force fields. Feedback control strategies of such virtual structures have only been developed for simple 2- and 3-craft systems thus far.[14,15] A related concept to the proposed electrostatic membrane structure is the Tethered Coulomb Structure (TCS) presented in Reference 16. Here the complex charged relative orbital motion is constrained through the use of very thin tethers interconnecting the charged nodes. The electrostatic force is used to create an inflationary pressure to ensure positive tether tension at all times. Thus, the TCS can essentially be considered as a larger scale, discrete element version of an Electrostatically Inflated MembraneStructure (EIMS). In contrast to the TCS, the EIMS differential orbital perturbations that drive charging requirements will be very different due to the larger mass of the TCS system (50-100 kg nodes), versus the sub-kilogram membrane structure mass considerations.

The challenge of controlling the potential of a body in space has been flight tested with successful results. The SCATHA (Spacecraft Charging at High Altitudes) experiment was one of the spaceflight experiments which demonstrated use of ion and electron guns to control spacecraft surface potential to 10-20 kV.[17,18] Even without active charging, spacecraft can charge up to many kilovolts in the plasma environment. The highest recorded natural charging event occurred on the ATS-6 spacecraft, reaching a potential of -19 kV during an eclipse period of the GEO orbit.[19] While the previous two examples are space missions with active charge control at geosynchronous altitudes, the SPEAR I mission is an example of a charging experiment at Low Earth Orbit (LEO). The SPEAR I mission employed active charging of test spheres in LEO with an altitude of approximately 350 km.[20] Using a capacitor, a positive potential of 45.3 kV was applied to two 10 cm radius spheres attached to a rocket body.[20] The current CLUSTER mission also employs active charge control through continuous charge emission to servo the spacecraft absolute potential to a desired near-zero charge level. The charge control of a spacecraft is, however, complicated by the presence of the plasma environment. While at geostationary altitudes the charge control can be achieved with low electrical power levels,[21] the relatively cold and dense plasma at low Earth orbits makes charge control more challenging. LEO applications would require more power, and the electrostatic field about a charged body is more quickly negated by the surrounding plasma charge.

Reference 7 introduces the electrostatic inflation concept and discusses approximate required electrostatic charge densities for maintaining inflation under compressive pressures of orbital perturbations was described. This paper focuses on the challenging question as to what potential, not charge density, is required to compensate for orbital perturbations. The potential to charge relationship of one body is influenced by the presence of another charged body, making the evaluation of the objects capacitance quite challenging. This paper explores approximate EIMS capacitance relationships across a range of surfaces areas and membrane distances. Numerical finite element simulations are employed to study the full electrostatic response and compare to the symplified analytical predictions.

II. Electrostatic Inflation Concept

The concept of electrostatic inflation is applicable for gossamer structures on spacecraft. To illustrate the concept, the James Webb Space Telescope, shown in Figure 2 is used as an example. The telescope has a large sunshield consisting of several layers of silicon-coated Kapton which is used to reflect the heat of the sun, keeping the telescope cool.[22] The layers of kapton are mechanically tensioned to maintain the desired shape. The electrostatic inflation concept is envisioned to support a similar layered structure, yet without the external tensioning system. The pressure to maintain shape is provided by repulsive forces between electrostatically charged layers. Before changing the electrostatic potential of the structure, there is no stiffness to the body to maintain a desired shape. When the absolute potential has been raised, the electrostatic charge distributed across a layered structure results in electrostatic forces acting between the layers of the conducting material. These forces act as inflation pressure, similar to gas inflation. Like a ram-air parachute, the layered structures are envisioned to have ribs between the layers to tension the structure, as seen in Figure 3.

The ribs are assumed to only be able to provide tensile forces between the layers of the structure. If compressive forces are applied, then the ribs are modeled to buckle immediately and no longer interact with the outer membranes. The investigation of required electrostatic charge or potential for inflation presented in this paper are limited to 2-

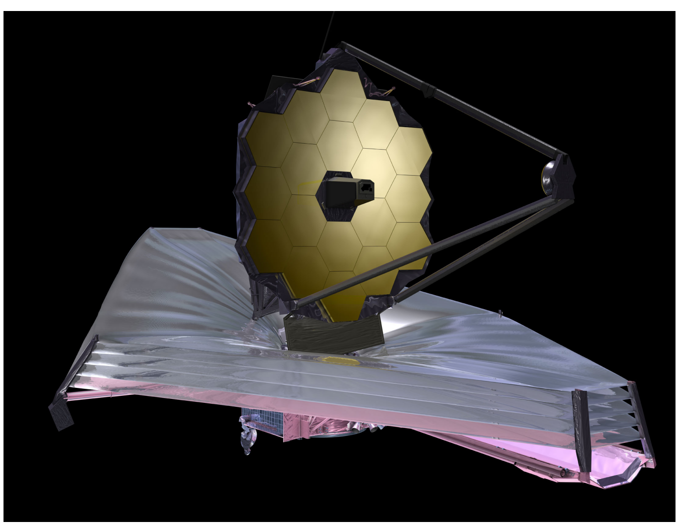

Figure 2: James Webb Space Telescope[22]

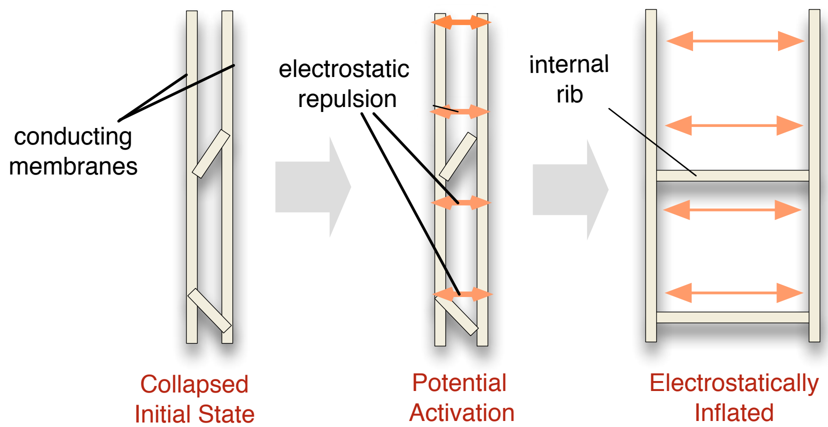

Figure 3: Sample open-ended membrane rib structure undergoing electrostatic inflation

layer gossamer structures in this sandwich-like configuration. Depending on the membrane material stiffness, such a sandwich structure would cause small amounts of pillowing between the ribs. Such effects are not considered in this first order study. Rather, this paper investigates what surface charge densities and resulting potentials are required on the membranes such that a sufficient electrostatic repulsion is achieved to overcome differential orbital perturbations. Future work will investigate higher order modeling of the complex membrane shape interactions with the disturbance forces, rib segments, space environment and the dominant electrostatic force fields.

In addition to the complexities of structural modeling, many other challenges to electrostatic inflation exist, such as plasma Debye shielding and the time varying space plasma environment, orbital perturbations, and complex electric fields. In the plasma environment of space, electrons and ions rearrange in the presence of a disturbing electric field to maintain macroscopic neutrality.[23] This phenomena, known as Debye shielding, will effectively shield the electrostatic field of a charged object in a plasma, such as an electrostatically inflated structure. In the Low Earth Orbit region, Debye lengths are typically on the order of milli- or centimeters, depending on the orbit altitude. If the separation distance between the layers of membrane in a gossamer structure in LEO is greater than a few centimeters, or of the order of the local Debye length, then the membranes may not experience a significant electrostatic force and the inflation concept would not be feasible. The details of the LEO plasma flows about a EIMS concept with strong Debye shielding are still being investigated. However, large membrane separation distances will become increasingly challenging in this orbit regime. In the GEO regime, the Debye length is generally on the order of hundreds of meters. The small separation distances between proposed membrane structures compared to the comparatively large Debye lengths yield nearly negligible effects from the shielding, and the field decreases proportional to the $1/r^2$ vacuum electrostatic field dropoff. This is true even for the very worst GEO plasma weather conditions being considered.

There are many challenges for electrostatic inflation that are beyond the scope of this paper. One challenging issue is the storage and deployment of the structure. In laboratory experiments to inflate a structure such the one illustrated in Figure 3, a non-conducting gap or layer between conducting surfaces is required for electrostatic inflation to occur. Without a gap, the layers of charged conducting sheets do not separate. For electrostatic inflation, it is speculated that non-conducting segments are needed between the conducting surfaces such as gaps or un-polarized dielectric layers. Understanding the physical mechanism between sticking layers remains as future work. In lab experiments, a small gap with air between surfaces has shown sufficient for inflation to occur. These results are discussed in the last section. The following work assumes that the two plates are already minimally separated such that electrostatic repulsion can occur. Of interest is the following: how does the electrostatic repulsion between the membranes vary with different sizes and separation distances, and what potentials are required to be able to overcome the differential orbital perturbations experienced either at GEO or LEO altitudes.

III. Space Weather Impact

A. Debye Shielding of Point Charges

In the plasma environment of space, electrons and ions rearrange in the presence of a disturbing electric field to maintain macroscopic neutrality.[23] This phenomena, known as Debye shielding, will effectively shield the electrostatic field of a charged object in a plasma, such as an electrostatically inflated structure. To determine the potential near a charged object in a plasma, the number density of charged particles must be known. An expression for the electron density and ion density are given in Eqs. (1),[23] where k is the Boltzmann constant, T is temperature, ϕ is the potential due to a charge, and n_0 is a constant particle density where $n_e(\infty) = n_i(\infty) = n_0$.

$$n_e = n_0 e^{\frac{e\phi}{kT_e}} \tag{1a}$$

$$n_i = n_0 e^{-\frac{e\phi}{kT_i}} \tag{1b}$$

Using these definitions for particle number densities, Poisson's equation is written as:

$$\nabla^2\phi = -\frac{\rho}{\epsilon_0} = \frac{n_0 e}{\epsilon_0}\left(e^{-\frac{e\phi}{kT}} - e^{\frac{e\phi}{kT}}\right) \tag{2}$$

This classical development continues under the assumption that potential energy of the field is much smaller than the kinetic energy of the particles, or $(e\phi \ll kT)$. With this assumption the simplified expression is yielded:

$$\nabla^2\phi = \frac{2}{\lambda_D}\phi \tag{3}$$

where the parameter, λ_D is a parameter known as the Debye Length. The Debye length describes the distance at which a charge is essentially shielded by the plasma if $(e\phi \ll kT)$ is true. The Debye length is determined by plasma conditions through:

$$\lambda_D = \left(\frac{\epsilon_0 kT}{n_e e^2}\right)^{\frac{1}{2}} \tag{4}$$

where e is the elementary charge. This particular form of the Debye length computation assumes that the negative plasma electrons dominate the electrostatic charge shielding. The simplified form of Poisson's equation has a well known analytical solution for the potential surrounding a point charge, q_1, (or a charged sphere with total charge q_1) in spherical coordinates given by:

$$\phi = \frac{k_c q}{r} e^{-\frac{r}{\lambda_D}} \tag{5}$$

The Debye shielded electrostatic force experiences by a 2nd point charge q_2 is derived using Equation (5):

$$F = \nabla\phi \cdot q = \frac{k_c q_1 q_2}{r^2} e^{-\frac{r}{\lambda_D}}\left[1 + \frac{r}{\lambda_D}\right] \tag{6}$$

While this force computation is only valid for point charges, and not the plate models considered in this paper, Eq. (6) provides insight into how the plasma Debye length can limit the electrostatic actuation. Equation (6) allows for quick analytical computation of the electrostatic force for a point charge or spherical body assumption, as no simple analytical expression describes the electrostatic force between two plates. Numerical analysis is quickly required as geometry becomes more complicated. The following discussions consider conditions under which the Debye shielding can be treated as negligible in regard to the electrostatic force computation. This can be achieved through either flying the electrostatically inflated membrane structures at particular orbit altitudes, or employing large potentials.

B. Orbit Regions Applicable for Electrostatic Inflation

Debye shielding affects the feasibility of using electrostatics in a plasma environment. In the Low Earth Orbit region, Debye lengths are typically on the order of milli- or centimeters, depending on the orbit altitude. Table 1 shows the extremes of Debye lengths experienced in LEO at an orbit altitude of approximately 350 m, as predicted by the International Reference Ionosphere model and reported in Reference 24.

In earlier work on Coulomb control of free-flying charged spacecraft, or the electrostatic inflation of TCS concepts over several meters, this aggressive Debye shielding prevented such concepts from being considered at LEO.[11,25] However, with the electrostatically inflated membrane structures, even with surface areas of multiple square meters, the electrostatic force only has to occur across the membrane gap layer separation distance d which can be on the order of centimeters. If the separation distance between the membrane layers of a sandwich structure in LEO is greater than a few millimeters or centimeters, or of the order of the local Debye length, then the membranes would

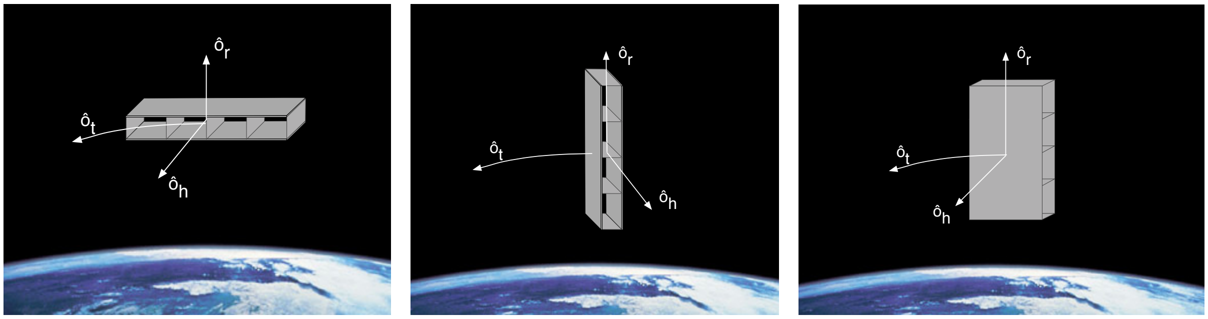

a) Radial Configuration **b)** Along Track Configuration **c)** Orbit Normal Configuration

Figure 4: Possible orbital configurations of the sandwich structure

not experience a significant electrostatic force and the inflation concept would not be feasible. This argument assumes that the membrane potential ϕ satisfies the condition that $(e\phi \ll kT)$. Thus, if small membrane gaps, d, less than of a centimeter are assumed, then even with the aggressive Debye shielding assumptions the electrostatic inflation could still occur at LEO. With the proposed concept it is not necessary for the electrostatic repulsion to occur between a membrane segment and the entire opposing membrane plate. Rather, the membrane structure provides some geometric stiffening through the tensioning membrane itself. Compared to earlier work on free-flying charged spacecraft where the formation size is directly limited by the electrostatic force drop off with separation distance, the membrane structure can scale to comparatively large dimensions as the electrostatic force does not need to act along the membrane width (w) and length (l) dimension, only across the much smaller separation (d).

In the GEO regime, the Debye length is generally on the order of hundreds of meters. However, these values can vary drastically with the solar storm activities heating up part of the plasma sheath, or pushing the lower and colder plasma pause conditions into the GEO altitudes.[26] The upper and lower bounds of possible geostationary Debye length values are shown in Table 1, as well as the nominal value. These Debye lengths are based on observations from the ATS-5 and ATS-6 spacecraft given in References 27 and 28. The small separation distances between proposed membrane structures compared to the comparatively large Debye lengths yield nearly negligible effects from the shielding, and the field decreases proportional to the $1/r^2$ vacuum electrostatic field dropoff. This is true even for the very worst GEO plasma weather conditions being considered.

Table 1: Range of Feasible Plasma Debye Lengths

	Smallest Debye Length	Nominal Debye Length	Largest Debye Length
LEO Environment	0.002 m	0.005 m	0.013 m
GEO Environment	4 m	200 m	743 m

IV. Orbit Perturbations Affecting Electrostatic Inflation

A. GEO Orbit Perturbations

For electrostatic inflation, potentials must be high enough to produce sufficient electrostatic inflation pressure for self-repulsion to negate the differential pressures from gravity, solar radiation pressure, and drag that would be experienced in orbit. These perturbations are all distributed over the surface of the structure. In the GEO environment, atmospheric drag is not a consideration, but differential gravity and solar radiation pressure are investigated. The effect of differential gravity depends on the orbit configuration as this perturbation will tension the structure in the radial configuration, compress the structure in the normal configuration, and have no effect in the along-track configuration.

The linearized differential gravity in the orbit radial configuration shown in Figure 4(a) is given by Equation (7) where μ is the gravitation parameter, r_c is the radius from Earth, and d is the separation distance of the membrane plates.[25] In this configuration the differential gravity force will aid in tensioning the structure, as the plate nearest to Earth will experience a stronger force due to gravity.

$$\delta F_{g,\text{radial}} \approx m\frac{3\mu}{r_c^3}d \tag{7}$$

For this study, mass is estimated from density, ρ and approximate material volume with area, A, and thickness, t:

$$m = \rho A t \tag{8}$$

75 gauge Aluminum coated Mylar, a possible material to be used for the proposed gossamer space structure, is used as the baseline material for this study. Thickness and density of this material are 19 microns and 1.40 g/cm^3, respectively. The mass contribution of the ribs is neglected here. To eliminate area dependence in the calculations, the differential pressure is calculated as follows:

$$\delta P_{g,\text{radial}} = \frac{\delta F_{g,\text{radial}}}{A} \approx \rho t \frac{3\mu}{r_c^3} d \tag{9}$$

For the along-track configuration shown in Figure 4(b) the differential gravity force and pressure are essentially zero:

$$\delta F_{g,\text{along-track}} \approx \delta P_{g,\text{along-track}} \approx 0 \tag{10}$$

In the orbit normal configuration in Figure 4(c), differential gravity will tend to compress the structure. The linearized differential gravity force in this configuration is given by Eq. (11).[25]

$$\delta F_{g,\text{normal}} \approx -m \frac{\mu}{r_c^3} d \tag{11}$$

Similarly, the differential gravity pressure is:

$$\delta P_{g,\text{normal}} = \frac{\delta F_{g,\text{normal}}}{A} \approx -\rho t \frac{\mu}{r_c^3} d \tag{12}$$

These differential gravity forces, however, are very small in comparison with the solar radiation pressure. This result differs from the perturbation analysis for Coulomb formation flying or tethered Coulomb structures in which the differential gravity has a much larger effect. The cause for this difference is that both separation distances and masses are orders of magnitude smaller for the gossamer 2-membrane rib structure.

The equation for the disturbance force from solar radiation pressure is given by:[29]

$$P_{SRP} = \frac{F_{SRP}}{A} = p_{SR} c_R \tag{13}$$

where

$$p_{SR} = 4.57e^{-6} \frac{N}{m^2} \tag{14}$$

is the nominal solar pressure at 1 AU from the sun, c_R is the reflectivity, and A is the area exposed to the sun. Note that the solar radiation pressure is independent of separation distance, area and orbit altitude. This pressure will therefore be identical at LEO and GEO orbits.

These GEO perturbations force magnitudes are next compared for the three configurations illustrated in Figure 5.

1. GEO Orbit Radial Configuration

The orbit radial configuration is defined as the large areas of each membrane to be nadir facing, as shown in Figure 5(a). Considering a worst case scenario, the solar radiation pressure would act directly normal to one plate. To avoid compression of the membrane structure, the inflationary electrostatic force must be greater than this differential solar radiation force. Figure 5(a) shows a comparison of the magnitudes of disturbing pressures experienced at GEO for the sandwich structure. Considering the disturbance pressures versus using the forces has the benefits that the disturbances per unit area can be considered. Thus, the following results are independent of the membrane structure area A. Note that the differential solar pressure dominates over the differential gravity even with large 1 meter separation distances. Again, this is in strong contrast to the research results on free-flying charged spacecraft where differential gravity terms dominate. With the membrane structures the area to mass ratio is significantly larger, allowing the solar radiation pressure to be orders of magnitude larger. As a result the tensioning ability of the radial differential gravity term provides negligible relief on the overall inflationary force requirement.

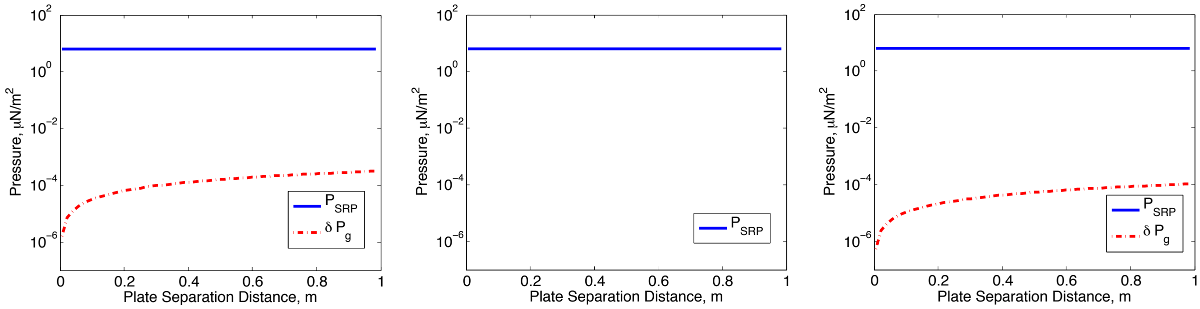

a) Radial Configuration **b)** Along Track Configuration **c)** Orbit Normal Configuration

Figure 5: Magnitudes of disturbance pressures in the radial, along-track, and normal configurations at GEO, mass $m = 0.01kg$

2. *GEO Along-Track Configuration*

In the along-track configuration, differential gravity has no effect on the sandwich structure. The only disturbance force is therefore solar radiation pressure, and the separation distance of the membranes will have no effect on the required electrostatic force for inflation. Again assuming a worst case alignment of the incident sun light with respect to the outer membrane surface, the resulting compressive solar radiation pressures are shown in Figure 5(b). Because this differential solar radiation pressure model is independent of the membrane separation distance, the minimum required inflationary pressure is a fixed value regardless of the sandwich structure thickness.

3. *GEO Orbit Normal Configuration*

Figure 5(c) shows a comparison of the magnitudes of disturbing pressures experienced at GEO for an inflated sandwich structure in the orbit normal configuration. These magnitudes are nearly identical to the radial configuration, with the exception that in the normal configuration, differential gravity tends to compress the structure instead of providing tension, as in the radial configuration. Again the solar pressure dominates the required inflationary force for this GEO configuration.

B. Perturbations in LEO

Next, let us consider a membrane structure which is flying at LEO altitudes. In addition to the differential gravity pressures and solar radiation pressure expressed in Equations (9), (12), and (13), the perturbation from atmospheric drag is also considered. The drag force at these altitudes cannot be neglected as a perturbation as it may be at GEO altitudes. The force on the leading plate is calculated with:[29]

$$F_D = -\frac{1}{2} C_D A \rho v_{rel}^2 \frac{\mathbf{v}_{rel}}{|\mathbf{v}_{rel}|} \tag{15}$$

Again, to eliminate area dependence, the differential pressure from drag is calculated with:

$$P_D = -\frac{1}{2} C_D \rho v_{rel}^2 \frac{\mathbf{v}_{rel}}{|\mathbf{v}_{rel}|} \tag{16}$$

This force, however, is only considered for the along-track configuration. Here the large area of one plate is bombarded by the rarified atmospheric particles, while the other plate is protected in the wake of the leading plate. The resulting differential drag force on the leading plate tends to compress the structure. In the orbit radial and normal configurations the differential drag forces are negligible as no significant area is be presented relative to the incoming rarified atmosphere. For the sandwich structure with an area of 0.5 m^2 and a mass of 0.01 kg, a study is performed to determine the altitude at which the drag force diminishes versus the differential solar radiation forces. Values for atmospheric density are calculated using the MSIS-E-90 Atmospheric Model.

As shown in Figure 6, below approximately 500km the atmospheric drag pressure is the dominating perturbation. Above this altitude, the density becomes too low to have an appreciable effect. Below this altitude, the required charge densities or potentials to inflate a membrane structure must take the differential atmospheric drag into careful consideration.

Figure 7 displays the magnitudes of differential gravity, solar radiation and drag pressures at a LEO altitude of 300 km. The differential gravity pressure is approximately two orders of magnitude larger at this altitude than at GEO.

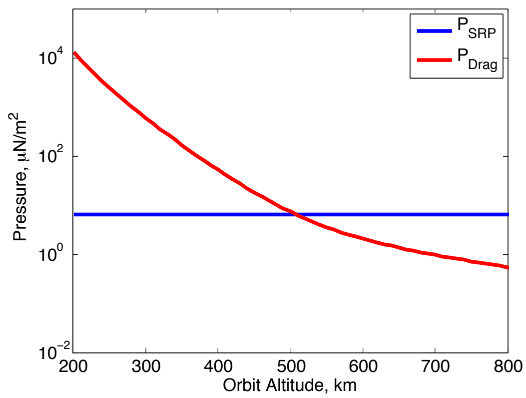

Figure 6: Disturbance pressures as a function of altitude in LEO

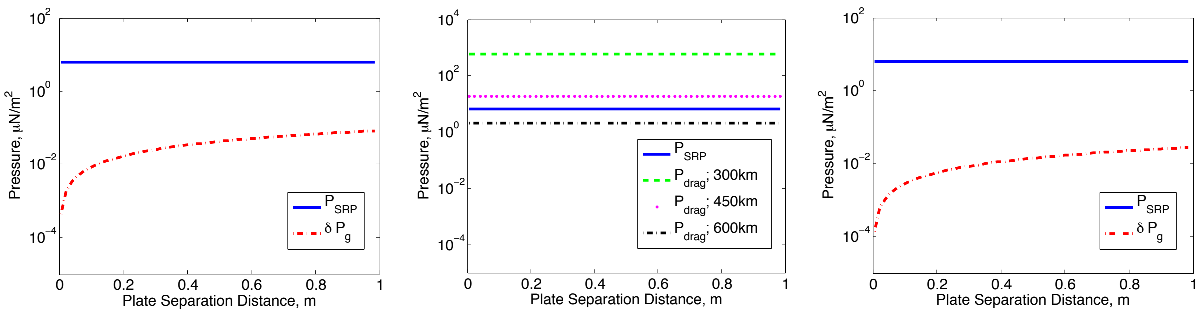

a) Radial Configuration **b)** Along Track Configuration **c)** Orbit Normal Configuration

Figure 7: Magnitudes of disturbance pressures in the radial, along-track, and normal configurations at LEO, mass $m = 0.01kg$, orbit altitude of 300 km with a range of altitudes shown for drag pressures

The solar radiation pressure, however, is the same at LEO as GEO due to the independence from orbit altitude. For the along-track configuration pressures, shown in Figure 7(b), the drag pressure is displayed at three different orbit altitudes to demonstrate the dramatic effect of orbit altitude on drag in LEO. As was illustrated in Figure 6, below 500 km, the drag pressure dominates the solar radiation pressure. This is seen again in Figure 7(b), as the drag pressure at 450 km is larger than the solar radiation pressure, but at 600 km, the solar radiation pressure has become dominant. At 300 km, the drag pressure dominates by two orders of magnitudes. Below 500 km, the drag force is clearly the perturbation that causes the largest effect and must be compensated for with sufficient electrostatic repulsion.

V. Minimum Electric Potentials to Offset Perturbations

Electrostatic inflation of a structure occurs when an electrostatic potential is applied and the charges distributed on the surface repel each other, expanding the structure. The potentials must be high enough to produce sufficiently larger electrostatic forces for self-repulsion to negate the differential forces from gravity, solar radiation pressure, and atmospheric drag that would be experienced in orbit. In Reference 7, the required charge densities to produce these repulsive pressures between membranes of simple electrostatically inflated structures to maintain a desired nominal shape after deployment are discussed. Voltage, however, is the quantity which will be actively controlled in the space environment to charge the structure, therefore must also be determined. As the structures are not simple shapes, such as a sphere or classical parallel plate capacitor, a relationship between the potential and charge is not analytically known. In the following section, the procedure for determining the voltage required for producing sufficient electrostatic inflation pressure to offset orbital perturbation pressures for a membrane sandwich structure is discussed. Numerical electrostatic field solvers allow the determination of the capacitance relationship between the charges densities and the required voltage. These results are discussed in the following subsections.

A. Electrostatic Force due to a Charged Membranes

Before discussing charge or voltage requirements, the electrostatic force on a charge due to a charged membrane must first be understood. Electrostatic fields are complicated by issues such as non-uniform charge distributions and edge effects, therefore require numerical field solvers for an accurate description. An approximation of the field at a distance from a charged membrane can be made using the equation for the field due to a finite rectangular plate:[30]

$$E = \frac{\sigma}{\pi\epsilon_0} \arctan\left(\frac{lw}{4d\sqrt{\left(\frac{l}{2}\right)^2 + \left(\frac{w}{2}\right)^2 + d^2}}\right) \tag{17}$$

Here σ is the surface charge density, while the plate dimensions w, l and d are illustrated in Figure 8.

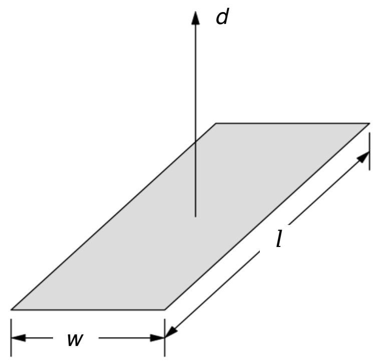

Figure 8: Definitions for rectangular plate field model

Note that the electrostatic field strength E in Eq. (17) is only valid moving along the rectangular plate center axis shown in Figure 8. The electrostatic force experienced by a charge above the center of a charged plate is therefore determined from Equations (17) and the fundamental electrostatic force equation:

$$F = Eq \tag{18}$$

When considering two membranes, the total force on one membrane can be approximated by assuming all charge of that membrane lies at a point above the center of the other membrane, as shown in Figure 9. The total charge on the membrane is found by assuming a constant surface charge density, σ, thus a total charge of σA. This allows the finite rectangular plate model to be used to approximate the total force between the two plates.

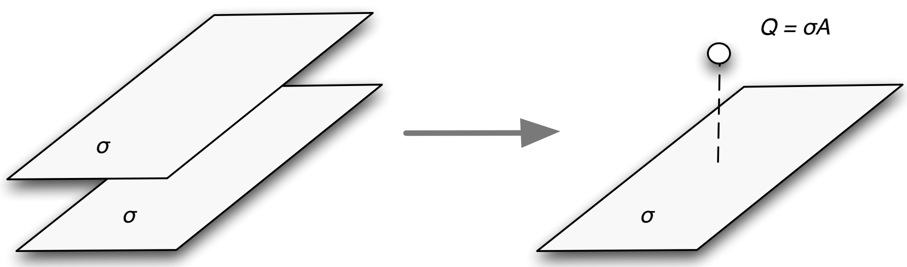

Figure 9: Approximation for total force on one membrane due to the opposing membrane by lumping total charge, Q

Assuming the charge density on each plate is equal, the force on each plate is determined as shown in Equation (19).

$$F = \frac{\sigma^2 A}{\pi\epsilon_0} \arctan\left(\frac{lw}{4d\sqrt{\left(\frac{l}{2}\right)^2 + \left(\frac{w}{2}\right)^2 + d^2}}\right) \tag{19}$$

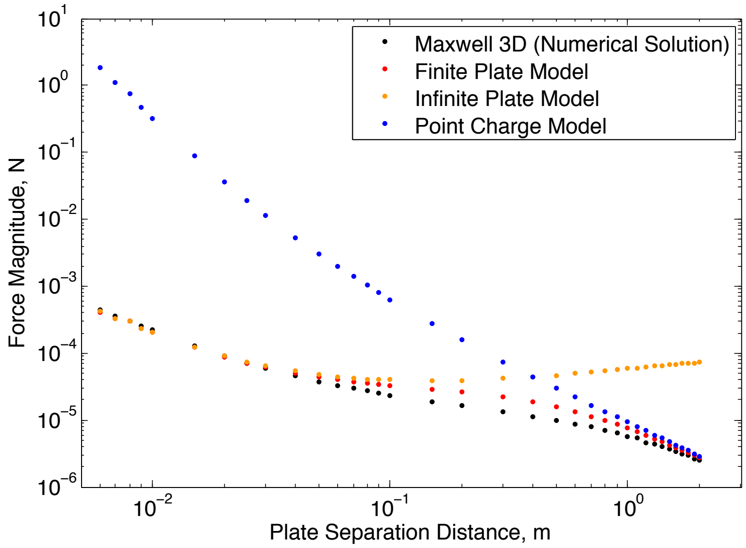

Figure 10: Numerical solutions of repulsive force between two charged plates compared with analytical force models; Membrane area $1m^2$, fixed Voltage of 1000 kV

The accuracy of this model is investigated by comparison to numerical results. A comparison of several models to the numerical solution of the force between two charged membranes is shown in Figure 10. For this comparison, the two plates are at a fixed potential of 1 kV with areas of $1m^2$. The approximation using the finite plate model is a close match to the numerical result, but over-predicts the force in the decimeter separation range. This is an effect of non-uniform charge distribution and the assumption of lumped charge in the finite-plate model. This will be later addressed. In the millimeter and centimeter range, the finite plate model is a close approximation to the numerical results. For the proposed Gossamer structures with square meters of surface areas, the membrane layer separation distance d is considered to be on the order of centimeters, therefore the finite plate model is assumed sufficient for the remainder of this first-order analysis as it captures the dominant electrostatic field. In Figure 10, the point charge model is shown to illustrate that as the plates reach a separation distance on the order of their length, the behavior begins to match the point charge (or spherical charged object) model. When the plates are only millimeters apart, their behavior matches the infinite plate model.

For this comparison of force models, numerical solutions of the capacitance relationship between voltage and charge were required. The numerical simulations are performed with the the Maxwell 3D numerical field solver software. Details of this relationship will be further explained in the section 'Capacitance Relationship for Two Plate Configuration.' The capacitance relationship was required as the input to the Maxwell 2D software is Voltage, while the analytical force models are a function of charge.

B. Charge Density Requirements

In the previous section, the magnitudes of disturbance pressures from differential gravity, solar radiation pressure and atmospheric drag are discussed for different orbit regimes and configurations of the membrane sandwich structure. For inflation of the structure, there must be sufficient electrostatic pressure across the entire surface of the membrane to offset these perturbations. This required pressure to exactly offset the disturbances will be associated with a required electrostatic charge density which is referred to as the minimum charge density on the membrane. Below this minimum charge density there could be collapse of the structure.

When considering the minimum charge density, it is important to consider the non-uniformity of the charge distribution on the membranes. The Maxwell 3D software has been used to aid in understanding the true charge distributions. Numerical results show that surface charge is highest at corners, as can be seen in Figure 11 where red represents the largest value of surface charge.

As seen in Figure 11, the minimum charge density is in the center of the membrane. The pressure at this location is therefore a quantity of interest. Consider the location of minimum charge density to occur on a small element of area dA_1 on membrane 1. The labeling of membrane 1 or 2 can be interchanged without loss of generality. The charge on

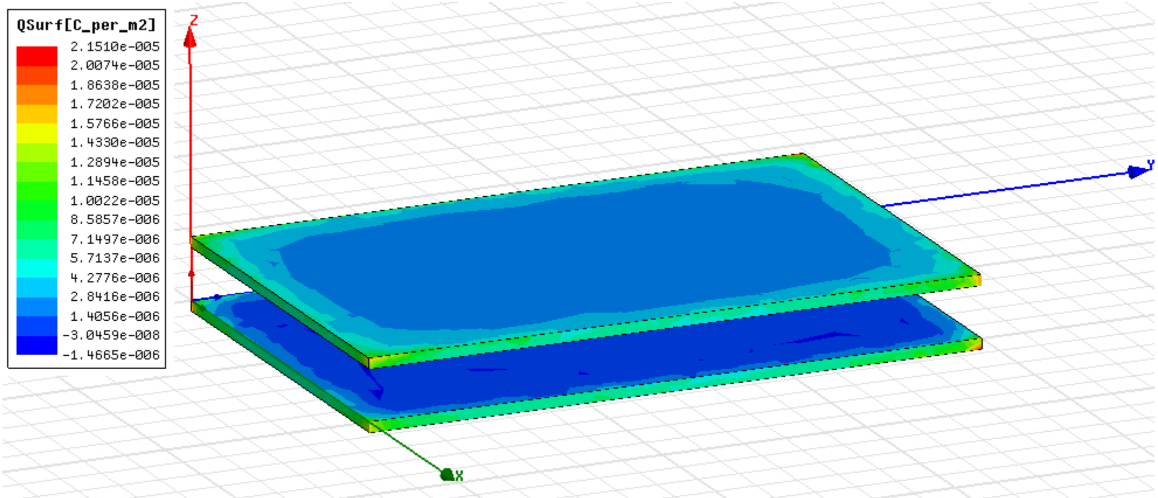

Figure 11: Numerical solutions of surface charge distribution on two charged plates

this differential area is:

$$\mathrm{d}q_1 = \sigma_1\,\mathrm{d}A_1 \tag{20}$$

The differential force on this area due to the opposing membrane (membrane 2) is:

$$\mathrm{d}F_1 = E_2 \mathrm{d}q_1 \tag{21}$$

where E_2 is simply the electrostatic field due to the other membrane, as given in Equation (17). Rewriting this equation as the pressure by dividing each side by area and substituting Equation (20) yields:

$$\mathrm{d}P_1 = \frac{\mathrm{d}F_1}{\mathrm{d}A_1} = \frac{E_2\sigma_1\mathrm{d}A_1}{\mathrm{d}A_1} = \sigma_1 E_2 \tag{22}$$

Substituting the electrostatic field of the finite plate yields:

$$\mathrm{d}P_1 = \frac{\sigma_1\sigma_2}{\pi\epsilon_0}\arctan\left(\frac{lw}{4d\sqrt{\left(\frac{l}{2}\right)^2 + \left(\frac{w}{2}\right)^2 + d^2}}\right) \tag{23}$$

Recall that Equation (23) hinges on the assumption that the charge density of membrane 2 is a uniform value of σ_2. If the same assumption is made for membrane 1, then these two densities will be equal ($\sigma_1 = \sigma_2 = \sigma$). With this

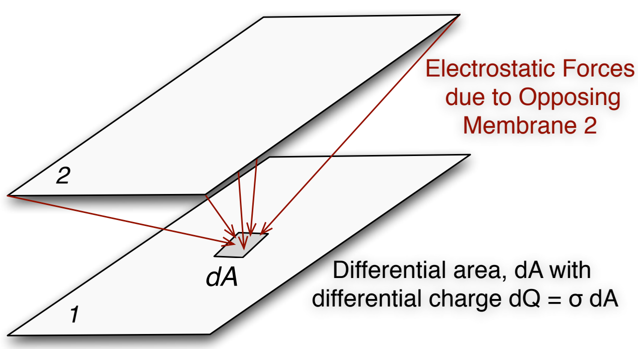

Figure 12: Differential area element experiencing electrostatic forces from the distributed charge on the opposing membrane

assumption, Equation (23) can be rearranged to solve for the charge density to create a required inflationary pressure level (P_{req}) which at least matched the differential pressure from orbital perturbations.

$$\sigma = \sqrt{\pi\epsilon_0 P_{\text{req}} / \arctan\left(\frac{lw}{4d\sqrt{\left(\frac{l}{2}\right)^2 + \left(\frac{w}{2}\right)^2 + d^2}}\right)} \tag{24}$$

where the required pressure is equal to the pressure on a differential area at the center of the membrane (as given in Equation (22)) and also equal to the sum of all orbital perturbation pressures.

$$P_{req} = dP_1 = P_{SRP} + P_D + P_g \tag{25}$$

What is of question, however is the location of minimum pressure, which will not necessarily be at the center of the rectangular membrane. When moving away from the z-location directly above the center of the other membrane, the force on charge will decrease (per Coulomb's law). There would therefore be a 'sweet spot' location of the minimum pressure that is a balance between lower charge density at the center of the plate and lower electrostatic force at the edge of the plate. Currently, work is being done to develop a more accurate model to that will incorporate the variations in charge distribution in the force model.

Equation (24) is now used to examine approximate required charge densities at GEO and LEO, assuming uniform charge distributions. In the along-track configuration (large membrane area facing the relative wind), the only differential perturbation in GEO is solar radiation pressure. This pressure is constant for any separation difference between the two membranes of the sandwich structure. Figure 13(a) shows the required charge densities in GEO to achieve inflation which will exactly offset the compression pressure due to solar radiation pressure, as calculated with Equation (24) and shown in Figure 5(b). A range of plate areas are shown as well as the infinite plate model, which is approached as membranes become very large in comparison to the membrane separation distance. Figure 13(b) shows these minimum required charge densities in LEO for a 300 km orbit altitude. As this orbit is below 500 km, the atmospheric drag is the largest perturbation. At this altitude, the required charge density is approximately an order of magnitude larger than what would be required for offsetting solar radiation pressure alone. For these separation distances and membrane sizes, the total charge on each plate of the sandwich structure remains in the range of or below microCoulomb levels in any orbit or configuration.

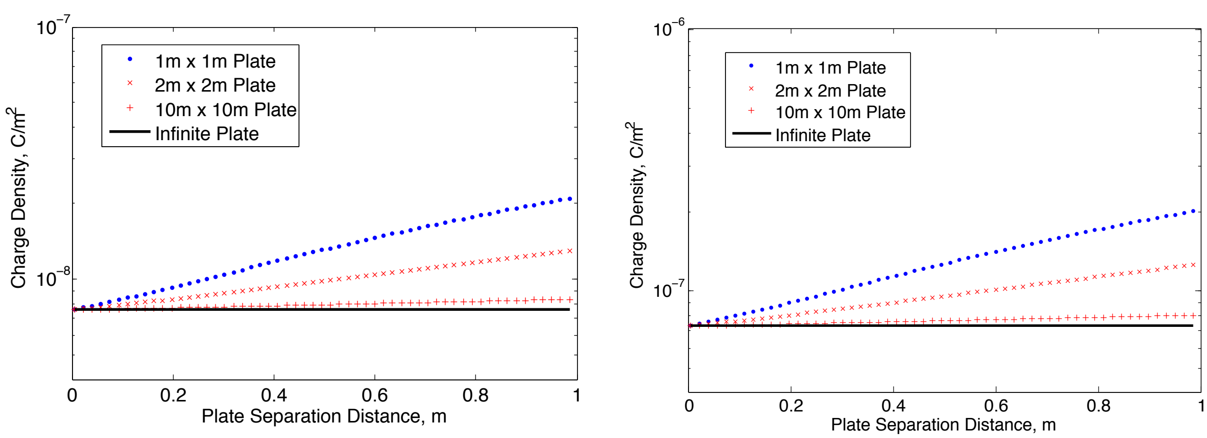

a) GEO Along Track Configuration

b) LEO Along Track Configuration, 300 km altitude

Figure 13: Minimum required surface charge density for electrostatic Inflation at GEO and LEO for a range of plate areas

C. Capacitance Relationship for Two Plate Configuration

What is of interest, however, is not just the charge, but the voltage which corresponds to the required charge density for maintaining inflation. As the sandwich structure is not a simple shape, such as a sphere, there does not exist an analytical capacitance relationship between the voltage and charge. Numerical electrostatic field modeling is necessary to determine the charge density to voltage relationship for the proposed sandwich membrane structures and other complicated structures.

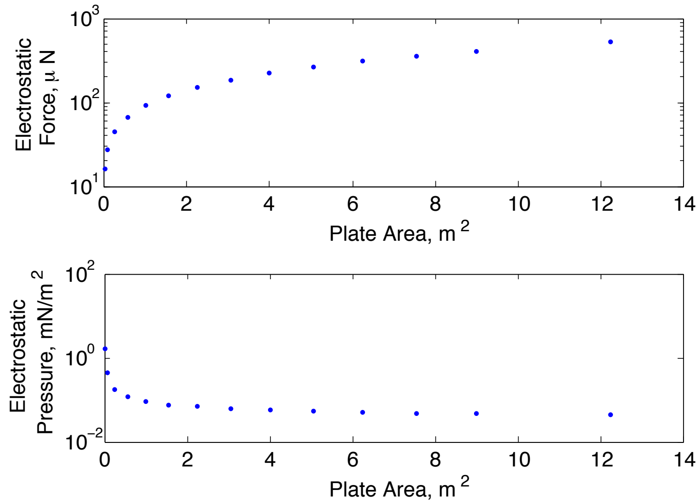

Figure 14: Numerical simulation of effect of varying structure area on the capacitance of the system, Fixed separation 2cm, Fixed potential 1 kV

To understand the capacitance relationship for the sandwich configuration, Ansoft's Maxwell 3D software[31] was used to create models, simulate electrostatic fields, and numerically solve for forces within the structure. The numerical simulations were performed for a model of two conducting, finite plates in a vacuum. For N capacitors, the capacitance matrix to relate the potential and total charge on the conductors is an NxN matrix. For the two plate configuration, the relationship is as shown in Equation (26). The diagonal components of this symmetric matrix are the capacity coefficients and the off-diagonal terms are the electrostatic induction coefficients.[32] The induction coefficients are negative values and account for the decrease in the potential due to a nearby conductor.

$$\begin{bmatrix} Q_1 \\ Q_2 \end{bmatrix} = \begin{bmatrix} C_{11} & C_{12} \\ C_{21} & C_{22} \end{bmatrix} \begin{bmatrix} V_1 \\ V_1 \end{bmatrix} \tag{26}$$

The values of the capacitance matrix are dependent only on the geometry of the conductors. For this system, the capacitance can be altered by changing the area of the plates or by changing the separation distance between the plates. Figure 14 illustrates the effect of changing the area of the structure. Increasing the area increases the capacitance of the system, allowing more charge to reside on the structure for a fixed value of potential. The repulsive forces between the two membranes therefore increase with this additional charge, as shown in the top plot of Figure 14. When the pressure is considered, however, the increase in area causes a decrease in electrostatic pressure. Pressure is the quantity in which we are most interested, not total force, as the distributed pressures of orbital perturbations must be offset across the whole area of the structure. This suggests that electrostatic inflation can be achieved more easily for small area structures. The effect of changing the area on the system capacitance diminishes as the areas become larger than a few square meters, and the effect of area change on electrostatic pressure has nearly settled by areas of $4m^2$. The effect of varying the separation distance on the capacitance matrix is very significant. Figure 15 illustrates the trends for a range of separation distances between membranes with a fixed potential and area. The electrostatic forces become larger as the two membranes are brought closer per Coulomb's law and because the system capacitance increases as two conducting bodies become closer. This result suggests that it will be most advantageous to have the two membranes very close. Small separation distances between membranes are also preferred when considering Debye Shielding, especially at LEO where Debye lengths can be close to the order of the separation distances considered here.

D. Voltage Requirements for Inflation

With the numerical results of the capacitance relationship, the approximate required voltage for inflation can be determined with Equation (26). To illustrate the results, an example of the required voltage for a sandwich structure with $1m^2$ membranes in the along-track configuration of a GEO orbit is considered.

To summarize the procedure, first the orbital perturbations for the GEO orbit and along-track orientation were determined. The differential pressure is then related to the required charge density through Equation (24). A Maxwell 3D model of the configuration is created and the capacitance matrix is found numerically. As the capacitance does not

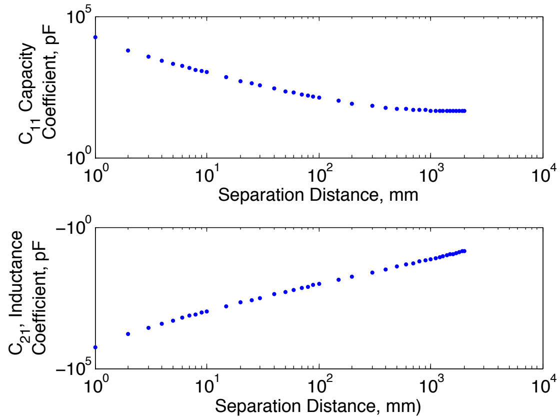

a) Capacitance of two plate system

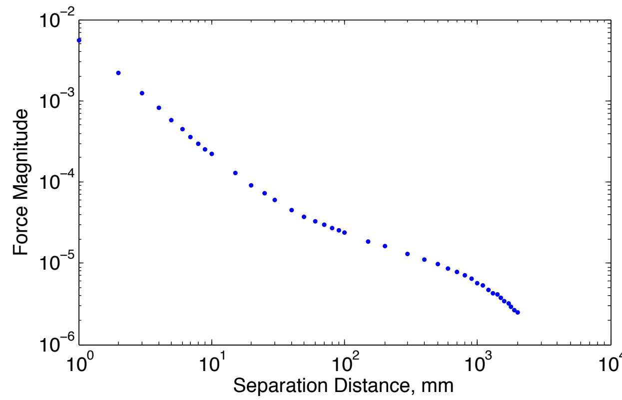

b) Electrostatic force between two plates

Figure 15: Numerical simulation of effects of varying separation distance between membranes; Fixed area of 1 m^2, Fixed potential $1kV$

depend on the potential of the membrane structures, any initial conditions for potential can be used. Assuming equal and uniform charge on each membrane surface, the capacitance matrix is used to determine the required voltage by inverting Equation (26):

$$[V] = [C]^{-1} [Q] \tag{27}$$

What is important to note here is that this model assumes a constant charge density across the plates. For a given configuration, an equilibrium charge density is found that exactly offsets the orbital pressures. However, with a non-uniform charge distribution, to have a value of this equilibrium charge density at the center of the membranes (where the least amount of charge physically occurs) requires higher charge densities in other regions of the membranes. This method therefore under-predicts the required voltage, as it does not account for the average charge density to actually be higher than the charge density at the center of the membrane. This is related to the result shown in Figure 10, where the analytical method over-predicted the force which would be experienced between the membranes. As the predicted force is too large, the required voltage is underestimated. The method, however, gives an approximate method to calculate required voltages analytically.

For the given orbit and configuration, the approximate potentials necessary to offset perturbing orbital pressures, per the method described above, are shown in Figure 16 for a range of membrane separation distances. From Figure

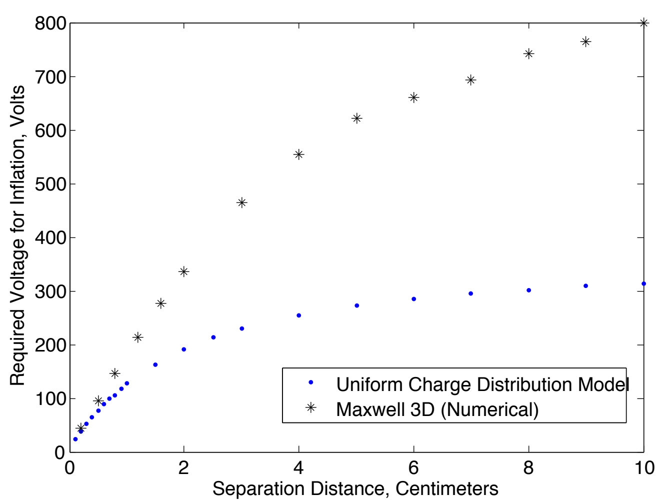

Figure 16: Required voltage for inflation at GEO of a sandwich structure for a range of separation distances; Area = 1 m^2

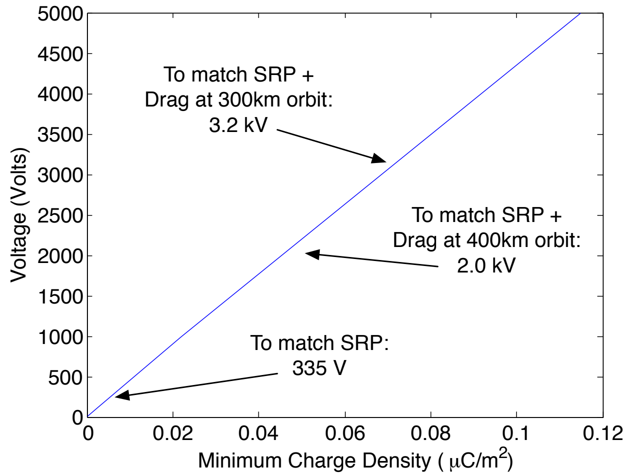

Figure 17: Numerical evaluation of the relationship between voltage the membranes and the minimum value of charge density (in the center of the membrane). Shown here for areas of $1m^2$ and a separation distance of $20mm$

16 it can be seen that the required potential is only on the order of a few hundred volts. This is a very small voltage compared to the kiloVolt levels that have been achieved through active charging in GEO. Even natural charging levels at GEO during eclipse can far exceed this level.

A more accurate method to assess the required voltage is to use the Maxwell 3D software to solve the full electrostatic field solution to understand the relationship between the voltage on the membrane to the minimum value of charge density. Maxwell 3D results for the minimum potential necessary to obtain the required charge density at the center of the membranes are also shown in Figure 16.

Also, the relationship between voltage and minimum charge density is shown in Figure 17 for two membranes with areas of $1m^2$ at a fixed separation distance of $20mm$.

Figure 17 shows that the relationship between these two parameters appears linear over the domain of voltages investigated. Comparing Figure 17 and Figure 16 also demonstrates the modeling error which is introduced by the simplified method of assuming a constant charge density across the membrane. For this example membrane configuration, the required voltage to offset SRP is 335 V. The analytical prediction yields 153 Volts. The under-prediction here is by approximately a factor of 2. Thus, using the uniform charge density assumption clearly leaves error in the final results of voltage requirements when using the analytical method. This reinforces the need for improved force modeling which will take into account the non-uniformity of the charge distribution. This method of determining voltages still yields required voltages within the order of magnitude of the numerical results which still remain hundreds of Volts range at GEO, which has been shown feasible by previous spacecraft missions.

It should be noted that the voltage that would be used to inflate the structure would be greater than just this equilibrium voltage. These results reflect a minimum that would be necessary to exactly offset orbital perturbations, but not provide any stiffness beyond this. Additional charging would be required to provide more stiffness, which would be especially desirable during attitude maneuvers which may deform the structure. What is important is that this analysis provides a good estimate of the order of magnitude of required potentials for inflation and these required potentials are feasible for charging in a GEO environment.

VI. Experimental Results

An experimental setup was designed to aid in testing and understanding the concept for electrostatic inflation. The setup consists of an aluminized Mylar ribbed sandwich structure resting on a conducting surface which is connected to a high voltage power source. Figure 18 shows the rib structure atop the conduction surface. In this 1-g test environment, the forces on the lower plate are always balanced by the normal force of the object upon which it rests. The other plate is subjected to the Coulomb force to inflate, the compressive force of gravity, and tension in the ribs to hold the structure together. This setup is much like the along track orbit configuration in which the differential solar radiation pressure and/or the differential atmospheric drag are acting on one plate to attempt to collapse the structure.

The structure used in the test shown in Figure 18 consists of two 12x15 cm plates of 75 gauge aluminized Mylar. Three ribs of the aluminized Mylar connect the two plates. Charge was applied to the conducting sphere on which the sandwich structure rested. In the sandwich structure inflation experiment, inflation occurred between 7 and 13 kV during different trials of the experiment. Figure 18 shows snapshots of the charging experiment. The duration of the inflation shown between the first and last frames of Figure 18 is approximately 5 seconds. This experiment clearly shows how a collapsed sandwich membrane structure can inflated with kilo-Volt levels of potential. It should be noted here that the rib structures were simply glued to the outer membrane plates. This results in some bending stiffness of the ribs that is not accounted for in the earlier models. Despite these challenges, the experiments indicate that such self-supporting membrane structures can repeatably and reliably be electrostatically inflated in a laboratory environment. Higher fidelity modeling of such lightweight structures is very challenging due to the strong nonlinear coupling between charge distribution and membrane shape. Adding the plasma space environment complicates the matter even further. Such experimental results are critical to explore experimentally appropriate material properties, construction methods, packing methods, and charging behaviors that lead to desirable membrane motions. Further, such testing will be used for validation and verification purposes of to be developed higher fidelity modeling of charged membrane structures.

Figure 19 shows the inflation of a gossamer ribbon structure, an example of a structure with large open surface segments. This ribbon structure was initially compacted to height of approximately 2 cm, then inflated to a height of 25 cm. This experiment shows the potential of high deployed to stowed volume ratios with the electrostatic inflation concept. Notice in this photo series that the structure has obtained the fully inflated shape at 5 kV, yet gravity is preventing the structure from standing upright. As the voltage increases to 9 kV, the electrostatic repulsion between the ribbon structure and the conducting surface to which it is attached cause the entire structure to become upright as well as inflated to the desired shape.

Considering effects such as membrane wrinkling and stiffness in the ribs will be important when analytically modeling inflation in future work. The glue used to construct the structure also contributes to additional stiffness. It is expected that the actual inflation voltage would be larger than can be predicted analytically.

The relatively small potential levels required to inflate the sandwich structure in 1-g are promising to the concept of electrostatic inflation for space structures. As the orbital disturbance pressures are orders of magnitude smaller than the pressure due to gravity in the 1-g environment, required potential will be much smaller than required in lab experiments. It is even possible that natural charging phenomena in orbit will provide sufficient potentials for inflating gossamer structures. However, note that this paper has focused on the minimum required charge densities to overcome differential perturbations. In practice, the Gossamer structure should be inflated to much larger values to provide

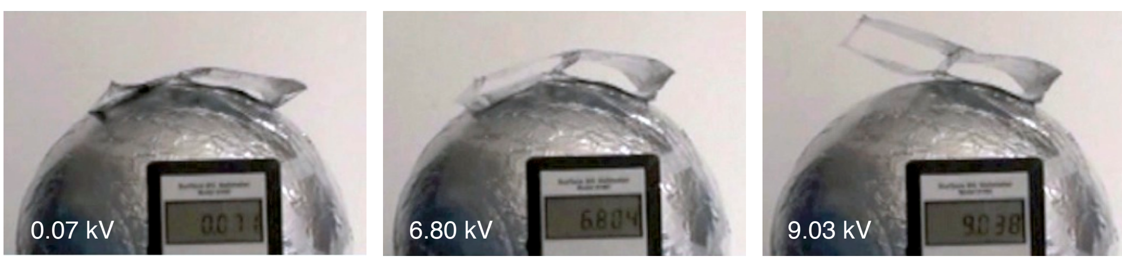

Figure 18: Electrostatic Inflation of a test sandwich structure, from 0 kV to 9 kV

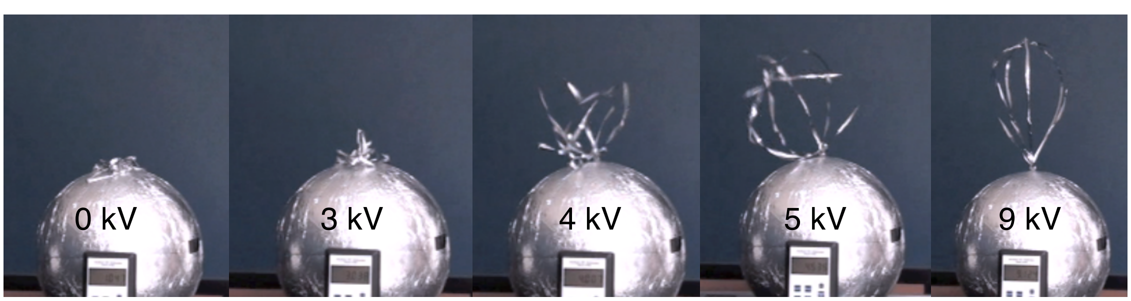

Figure 19: Electrostatic Inflation of gossamer ribbon test structure, from 0 kV to 9 kV

increased resistance to deformations.

VII. Conclusion

The focus of this paper is a study on the required potentials of space structures to maintain shape and stiffness. The potentials must be high enough to produce sufficient electrostatic forces to fight the differential forces from gravity, solar radiation pressure, etc that would be experienced in orbit. In GEO, the differential solar radiation pressure is the dominant perturbation. At LEO, atmospheric drag becomes dominant below approximately 500 km. Determination of differential orbital pressures allows calculation of the required charge densities for inflation. To determine these required potentials, the Maxwell 3D software was used to numerically solve for the relationship between charge and potential on a two-membrane sandwich structure. For a $1x1$ m^2 structure in GEO, it was found that only hundreds of volts are needed to offset orbital perturbations. Active and even passive charging at GEO have far exceeded this number on several spacecraft. These determined potentials serve as a minimum and larger values would be desirable to provide additional stiffness to the structure, but even these minimum values are orders of magnitude smaller than what has ben achieved on previous missions. Future work includes developing improved force models which account for non-uniformity of the charge distribution and also expressions to calculate forces away from the center of the opposing membrane, including Debye shielding, and accounting for structural deformations such as pillowing and wrinkling.

References

[1]Freeland, R. E., Bilyeu, G. D., , Veal, G. R., and Mikulas, M. M., "Inflatable Deployable Space Structures Technology Summary," *49th International Astronautical Congress*, Melbourne, Australia, Sept. 28 – Oct. 2 1998.

[2]Freeland, R. E., Bilyeu, G. D., Veal, G. R., Steiner, M. D., and Carson, D. E., "Large Inflatable Deployable Antenna Flight Experiment Results," *Acta Astronautica*, Vol. 41, No. 4–10, 1997, pp. 267–277.

[3]Banik, J. A. and Murphy, T. W., "Synchronous Deployed Solar Sail Subsystem Design Concept," No. AIAA-2007-1837, 47th AIAA Structures, Dynamics, and Mechanics of Materials Conference, 2007.

[4]Cadogan, D. P., Lin, J. K., and Grahne, M. S., "Inflatable Solar Array Technology," No. AIAA-99-1075, 37t hAIAAAerospaceSciences Meeting and Exhibit, 1999.

[5]Cadogan, D. P., Stein, J., and Grahne, M. S., "Inflatable Composite Habitat Structures for Lunar and Mars Exploration," *Acta Astronautica*, Vol. 44, 1999, pp. 399–406.

[6]Jenkins, C. H. M., editor, *Gossamer Spacecraft: Membrane and Inflatable Structures Technology for Space Applications*, Vol. 191 of *Progress in Astronautics and Aeronautics*, American Institute of Aeronautics and Astronautics, 2001.

[7]Stiles, L. A., Schaub, H., Maute, K. K., and Daniel F. Moorer, J., "Electrostatic Inflation of Membrane Space Structures," AAS/AIAA Astrodynamics Specialist Conference, Toronto, Canada, Aug. 2010.

[8]Cover, J. H., Knauer, W., and Maurer, H. A., "Lightweight Reflecting Structures Utilizing Electrostatic Inflation," US Patent 3,546,706, October 1966.

[9]MacEwen, H. A., editor, *Stretched Membrane with Electrostatic Curvature (SMEC) Mirrors*, Vol. 4849. SPIE, December 2002.

[10]King, L. B., Parker, G. G., Deshmukh, S., and Chong, J.-H., "Spacecraft Formation-Flying using Inter-Vehicle Coulomb Forces," Tech. rep., NASA/NIAC, January 2002.

[11]Schaub, H., Parker, G. G., and King, L. B., "Challenges and Prospect of Coulomb Formations," *Journal of the Astronautical Sciences*, Vol. 52, No. 1–2, Jan.–June 2004, pp. 169–193.

[12]Berryman, J. and Schaub, H., "Analytical Charge Analysis for 2- and 3-Craft Coulomb Formations," *AIAA Journal of Guidance, Control, and Dynamics*, Vol. 30, No. 6, Nov.–Dec. 2007, pp. 1701–1710.

[13]Schaub, H., Hall, C., and Berryman, J., "Necessary Conditions for Circularly-Restricted Static Coulomb Formations," *Journal of the Astronautical Sciences*, Vol. 54, No. 3–4, July-Dec. 2006, pp. 525–541.

[14]Natarajan, A. and Schaub, H., "Linear Dynamics and Stability Analysis of a Coulomb Tether Formation," *AIAA Journal of Guidance, Control, and Dynamics*, Vol. 29, No. 4, July–Aug. 2006, pp. 831–839.

[15]Wang, S. and Schaub, H., "Switched Lyapunov Function Based Coulomb Control of a Triangular 3-Vehicle Cluster," *AAS/AIAA Astrodynamics Specialist Conference*, Pittsburgh, PA, Aug. 9–13 2009.

[16]Seubert, C. R. and Schaub, H., "Tethered Coulomb Structures: Prospects and Challenges," *Journal of the Astronautical Sciences*, Vol. 57, No. 1-2, Jan.–June 2009, pp. 347–368.

[17]McPherson, D. A., Cauffman, D. P., and Schober, W., "Spacecraft Charging at High Altitudes - The SCATHA Satellite Program," *AIAA Aerospace Sciences Meeting*, Pasadena, CA, Jan. 20–22 1975.

[18]Mullen, E. G., Gussenhoven, M. S., Hardy, D. A., Aggson, T. A., and Ledley, B. G., "SCATHA Survey of High-Voltage Spacecraft Charging in Sunlight," *Journal of the Geophysical Sciences*, Vol. 91, No. A2, 1986, pp. 1474–1490.

[19]Olsen, R. C., "Record Charging Events from Applied Technology Satellite 6," *J. Spacecraft*, Vol. 24, No. 4, 1986, pp. 362–366.

[20]Katz, I., "Structure of the Bipolar Plasma Sheath Generated by SPEAR I," *Journal of Geophysical Research*, Vol. 94, No. A2, Feb. 1989, pp. 1450–1458.

[21]King, L. B., Parker, G. G., Deshmukh, S., and Chong, J.-H., "Study of Interspacecraft Coulomb Forces and Implications for Formation Flying," *AIAA Journal of Propulsion and Power*, Vol. 19, No. 3, May–June 2003, pp. 497–505.

[22]"James Webb Space Telescope," Mar. 2011.

[23]Bittencourt, J. A., *Fundamentals of Plasma Physics*, Springer, 3rd ed., 2004.

[24]Hastings, D. E. and Garrett, H. B., *Spacecraft-Environment Interactions*, Cambridge University Press, 1996.

[25] Seubert, C. R. and Schaub, H., "Tethered Coulomb Structures: Prospects and Challenges," *AAS F. Landis Markley Astrodynamics Symposium*, Cambridge, MA, June 30 – July 2 2008, Paper AAS 08–269.

[26] Pierrard, V., Goldstein, J., André, N., Jordanova, V., Kotova, G., Lemaire, J., Liemohn, M., and Matsui, H., "Recent Progress in Physics-Based Models of the Plasmasphere," *Space Science Reviews*, Vol. 145, No. 1, 05 2009, pp. 193–229.

[27] Garrett, H. B. and DeForest, S. E., "An Analytical Simulation of the Geosynchronous Plasma Environment," *Planetary Space Science*, Vol. 27, 1979, pp. 1101–1109.

[28] Lennartsson, W. and Reasoner, D. L., "Low-Energy Plasma Observations at Synchronous Orbit," *Journal of Geophysical Research*, Vol. 83, No. A5, 1978, pp. 2145–2156.

[29] Vallado, D. A., *Fundamentals of Astrodynamics and Applications*, Space Technology Library, Springer, 3rd ed., 2007.

[30] Hobbie, R., *Intermediate Physics for Medicine and Biology*, Springer, 3rd ed., 1997.

[31] Ansoft, *User's Guide: Maxwell 3D*, 11th ed., Jan. 2010.

[32] Landau, L. D. and Lifshitz, E. M., *Electrodynamics of Continuous Media*, Vol. 8 of *Course of Theoretical Physics*, Addison-Wesley Publishing Company, Inc., 1960.